WAVES IN MEDIA WITH VARIABLE AND CONSTANT BULK VISCOSITY

A. G. Lyakhov, G. M. Lyakhov, and V. N. Okhitin UDC 624.131 + 532.529

Wave problems were solved in [1-3] with a model of a multicomponent inviscid medium, and in [4-7] with a constant bulk viscosity η.

We solve here the problem of the propagation of a plane one-dimensional wave generated by impact loading and by a continuously increasing load in a multicomponent medium with $\eta = 0$ (inviscid medium), $\eta = \eta_0$ (constant viscosity), and $\eta = \eta(\varepsilon)$ (viscosity varying with the deformation of the medium). A comparison of the solutions obtained permits a determination of the effect of a change in η on the laws of wave propagation.

Wave processes in liquids containing gas bubbles, and in water-saturated soil (a medium consisting of solid particles, liquid, and gas) where the gas is entrapped in the form of individual bubbles, are treated by using a model of a multicomponent medium with bulk viscosity [6]. The behavior of the medium is described by the equation

$$\frac{\dot{V}}{V_0} = \varphi(p)\dot{p} - \frac{\alpha_1}{\eta}\psi(p, V), \tag{1}$$

where p is the pressure in the medium, V and V_0 are the specific volumes at pressure p and atmospheric pressure p_0, $\varphi(p) = (dV_D/dp)/V_0$, and $V_D(p)$ is the dynamic compression diagram of the medium as $\dot{p} \to \infty$, $\dot{V} \to \infty$. The function $\psi(p, V) = 0$ corresponds to the static compression diagram of the medium (equilibrium diagram) as $\dot{p} \to 0$, $\dot{V} \to 0$, and η is the bulk viscosity.

In this case

$$\frac{V_D}{V_0} = \alpha_1 + \sum_{i=2}^{3} \alpha_i \left[\frac{\gamma_i (p - p_0)}{\rho_{i0} c_{i0}^2} + 1\right]^{-\frac{1}{\gamma_i}}; \tag{2}$$

$$\psi(p, V) = p - p_0 \alpha_1^{\gamma_1} \left\{\frac{V}{V_0} - \sum_{i=2}^{3} \alpha_i \left[\frac{\gamma_i (p - p_0)}{\rho_{i0} c_{i0}^2} + 1\right]^{-\frac{1}{\gamma_i}}\right\}^{-\gamma_1}, \tag{3}$$

where i is the number of the component: the first is gas, the second liquid, and the third solid particles; α_i is the volume content of the i-th component; $V_{i_0} = 1/\rho_{i_0}$ is the specific volume, and c_{i_0} is the speed of sound in the i-th component at $p = p_0$. In a liquid–gas medium $\alpha_3 = 0$.

It is assumed in the model that in the free state all the components are compressed according to the equation

$$p - p_0 = \frac{\rho_{i0} c_{i0}^2}{\gamma_i}\left[\left(\frac{V_{i0}}{V_i}\right)^{\gamma_i} - 1\right]. \tag{4}$$

This equation corresponds to a Poisson adiabat for the gas and Tait's equation for water and the material of the solid component. It is assumed that the liquid and solid components of the medium are compressed instantaneously during loading according to this same equation, and the gas gradually as the volume of the bubbles is filled by the remaining components. In this case

$$p - p_0 = \frac{\rho_{10} c_{10}^2}{\gamma_1}\left[\left(\frac{V_{10}}{V_1}\right)^{\gamma_1} - 1\right] - \eta \frac{\dot{V}_1}{V_{10}}.$$

Moscow. Translated from Zhurnal Prikladnoi Mekhaniki i Tekhnicheskoi Fiziki, No. 3, pp. 103-109, May-June, 1981. Original article submitted February 28, 1980.

As $\eta \to 0$ and $\eta \to \infty$ Eq. (1) goes over into the compressibility equations of an inviscid medium, with the compression diagrams coinciding with the static and dynamic compression diagrams of a viscous medium.

The value of η is found experimentally. An approximate value of η can be found by making certain assumptions about the character of the deformation of the gas bubbles. All the bubbles are assumed spherical and of the same radius.

When the pressure p_B within a bubble is instantaneously balanced, the rate of change of its volume V_B is

$$\dot{V} = -4\pi r^2 u_B, \quad V_{B0} = 4\pi r_0^3/3, \quad \frac{\dot{V}_1}{V_{10}} = \frac{\dot{V}_B}{V_{B0}} = -\frac{3u_B}{r_0}\left(\frac{r}{r_0}\right)^2,$$

where u_B is the rate of displacement of the surface of the bubble toward the center, r_0 is its initial radius, and r is the running radius.

In accord with Eqs. (1)-(3), at each instant

$$\frac{V}{V_0} = \sum_{i=1}^{3} \alpha_i \frac{V_i}{V_{i0}}, \quad \frac{\dot{V}}{V_0} = -\frac{3\alpha_1 u_B}{r_0}\left(\frac{r}{r_0}\right)^2 + \sum_{i=2}^{3} \alpha_i \frac{\dot{V}_i}{V_{i0}} = -\frac{3\alpha_1 u_B}{r_0}\left(\frac{r}{r_0}\right)^2 + \varphi(p)\dot{p}, \tag{5}$$

$$u_B = \frac{\psi(p, V) r_0}{3\eta}\left(\frac{r_0}{r}\right)^2.$$

The pressure within a bubble varies according to a Poisson adiabat. Hence

$$p_B = p_0\left(\frac{V_{10}}{V_1}\right)^{\gamma_1} = p_0 \alpha_1^{\gamma_1}\left(\frac{V}{V_0} - \sum_{i=2}^{3} \alpha_i \frac{V_i}{V_{i0}}\right)^{-\gamma_1} = p - \psi(p, V), \tag{6}$$

$$u_B = \frac{(p - p_B) r_0}{3\eta}\left(\frac{r_0}{r}\right)^2.$$

The initial escape velocity $u_{B0} = (p - p_B)r_0/3\eta$ can be calculated by using the theory of random collapse, as in the plane one-dimensional case. A rarefaction wave is propagated in the medium surrounding the bubbles where the pressure is p; a shock wave is propagated in air where the pressure $p_0 < p$. Flow in a rarefaction wave is described by the Riemann solution of the fundamental equations of motion. In this case

$$u_{B0} = \pm \int \sqrt{-\frac{dV}{dp}}\, dp + \text{const}.$$

V(p) is the compressibility law of the medium. The constant is determined from the conditions at the rarefaction wave front.

In air the pressure is the same as at the wave front where the relations

$$u_{B0} = \sqrt{(p - p_0)(V - V_0)}$$

are satisfied at the jump. V(p) is the Hugoniot adiabat.

The values of p_B and u_{B0} are determined from the matching condition for the rarefaction and shock waves.

By linearizing the Hugoniot adiabat and the compressibility equation of the medium surrounding the bubbles we find

$$u_{B0} = \frac{p - p_B}{A_2}, \quad \frac{p_B}{p_0} = \frac{A_1 p + A_2 p_0}{p_0(A_1 + A_2)}. \tag{7}$$

For a liquid—air medium $A_1 = \rho_{10}c_{10}$, and $A_2 = \rho_{20}c_{10}$. The value of p_B is close to p_0. For example, when $p/p_0 = 100$ for a water—air medium, $p_B = 1.02\ p_0$, which also justifies the linearization of the Hugoniot adiabat. The compressibility of the liquid is close to linear.

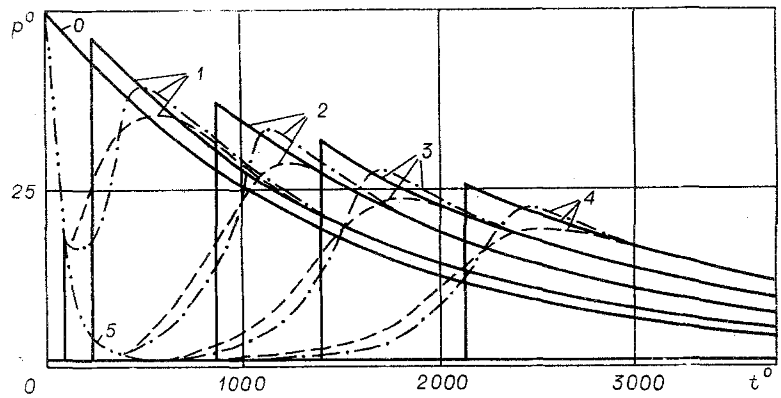

Fig. 1

From (6) and (7) we find the initial value of the viscosity

$$\eta_0 = A_2 r_0/3.$$

For a three-component medium the acoustic resistance A is determined by taking account of the contents of the liquid and solid components and their compressibilities.

During the compression of the medium the bubble radius can become smaller than the radius r^* corresponding to the equality of the external pressure p and the internal pressure p_B. Equilibrium is reached after some oscillations. The amplitude of the pressure oscillations due to pulsations of the bubbles is one or two orders of magnitude smaller than the wave amplitude [8, 9]. We therefore neglect the effect of pulsations and assume that there is a monotonic decrease of the radius from r_0 to r^*, and of the difference $p - p_B$ and the velocity u_B from maximum values to zero. We assume that the relation between $p - p_B$ and u_B remains approximately linear $p - p_B = A_2 u_B$. Then in accord with (6) we find

$$\eta = (A_2 r_0/3)(r_0/r)^2. \quad (8)$$

The viscosity at first increases, and after the equilibrium state is reached it decreases to the initial value.

Experiments on the propagation of compression waves in glycerin containing gas bubbles [8, 9] confirm the applicability of this model.

We compare the solutions for zero, finite (constant), and variable η.

We use Lagrangian variables x and t. The fundamental equations of motion of a continuous medium are

$$\frac{\partial u}{\partial x} - \rho_0 \frac{\partial V}{\partial t} = 0, \quad \frac{\partial u}{\partial t} + \frac{1}{\rho_0} \frac{\partial p}{\partial x} = 0.$$

This system is closed by Eq. (1). A wave is generated by loading in the cross section x = 0. We consider two types of loading:

impact

$$\begin{cases} p = p_0 + p_m \exp(-t/\theta) & \text{for} \quad t \geqslant 0, \\ p = p_0 & \text{for} \quad t \leqslant 0; \end{cases} \quad (9)$$

continuously varying

$$\begin{cases} p = p_0 + p_m \sin(\pi t/\theta) & \text{for} \quad 0 \leqslant t \leqslant \theta, \\ p = p_0 & \text{for} \quad t < 0 \text{ and } t > \theta. \end{cases} \quad (10)$$

The boundary condition at the wave front where the viscosity has no effect is

$$p - p_0 = \rho_0 u D, \quad (\rho - \rho_0) D = \rho u.$$

The system of equations is hyperbolic. The characteristic relations have the form

$$dp \pm (-V_0 \varphi(p))^{-1/2}\, du = \Phi(p, V) dt \text{ for } \pm (-V_0/\varphi(p))^{1/2} = \dot{x},$$
$$dp + (V_0 \varphi(p))^{-1} dV = \Phi(p, V) dt \text{ for } 0 = \dot{x},$$

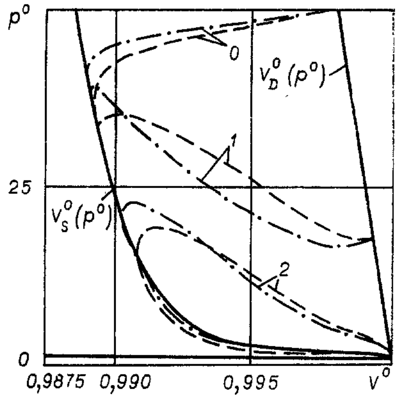

Fig. 2

where $\Phi(p, V) = \alpha_1\psi(p, V)/\eta(p, V)\varphi(p)$.

The solution was obtained by computer, using the method of characteristics for a water-air medium with an air content $\alpha_1 = 0.01$ and 0.1. The following values were used in the calculations: $\rho_{10} = 1.29$, $\rho_{20} = 10^3$ kg/m^3, $c_{10} = 330$, $c_{20} = 1500$ m/sec, $\gamma_1 = 1.4$, $\gamma_2 = 7$. The dimensionless variables $x^0 = x/r_0$, $t^0 = tc_{20}/r_0$, $p^0 = p/p_0$, $V^0 = V/V_0$, $\theta^0 = \theta c_{20}/r_0$.

Let us consider the results of calculating the parameters of a wave generated by impact loading in the form (9) for $p^0 = 50$, $\theta^0 = 1400$, and $\alpha_1 = 0.01$. Figure 1 shows the time dependence of the pressure in cross sections of the medium where x^0 is equal to 0, 100, 350, 550, and 800 (curves 0-4 respectively; curve 5 is the pressure in the precursor). From now on, dashed curves are for the pressure in a medium with variable η, dash-dot curves for a constant $\eta = \eta_0$, and solid curves for an inviscid medium.

In viscous media near the initial cross section the wave includes a jump beyond which there is a decrease of pressure, and after this a new gradual increase to a second maximum and a new decrease. The presence of two maxima can be observed already at a distance x^0 = 100 (curve 1). At large distances beyond the jump there is a continuous increase in pressure, and a decrease — the wave has one maximum. At still larger distances the jump disappears, and the pressure increases and decreases continuously. The magnitude of the pressure at the jump is the same for constant and variable η. However, the maximum pressure for a variable η is smaller, and the rate of damping of the wave is increased. Taking account of a variable η leads also to an increase in the time between the arrival of the beginning of the disturbance (jump) and its maximum, i.e., to a faster smearing of the wave.

In an inviscid medium the wave is a shock wave at all distances. The maximum pressure is higher than in viscous media. The pressure differences in the three cases being compared are of the order of 0.1 p.

Figure 2 shows compression and unloading p(V) curves in various cross sections of the medium during the passage of a wave. Curves 0-2 refer to distances x^0 = 0, 100, and 800 respectively; $V_D{}^0(p^0)$ and $V_S{}^0(p^0)$ are the dynamic and static compression diagrams of the medium. For an inviscid medium the state jumps down from the initial point on the $V_S{}^0(p^0)$ diagram, and as the pressure is decreased it returns along this same curve to the initial point. In viscous media with constant and variable η, the state drops from the initial point on the $V_D{}^0(p^0)$ diagram, which corresponds to the jump on the precursor. Then it proceeds on the static diagram and further beyond it. When the jump disappears the state proceeds directly on the static diagram. As the pressure decreases, the state approaches the initial point, remaining beyond the $V_S{}^0(p^0)$ curve. There is only a small difference between the p(V) curves for constant and variable η. Taking the radius of a bubble $r_0 = 0.1$ cm and $\theta^0 = 1400$, the dimensional time of action of the load in the initial cross section is $\theta = 0.93 \times 10^{-3}$ sec. Thus, for a loading lasting ~10^{-3} sec and a maximum pressure $p = 50 \times 10^5$ N/m^2 the state of the medium proceeds on the static diagram.

Figure 3 shows the time dependence of the pressure during the passage of a wave in the cross sections where x^0 = 0, 50, 100, 200, and 350 (curves 0-4 respectively) under impact loading (9) with $p^0 = 50$ and $\theta^0 = 1400$, but with a larger air content ($\alpha_1 = 0.1$) than in the preceding case (curve 5 is the pressure in the precursor). The differences between the maxi-

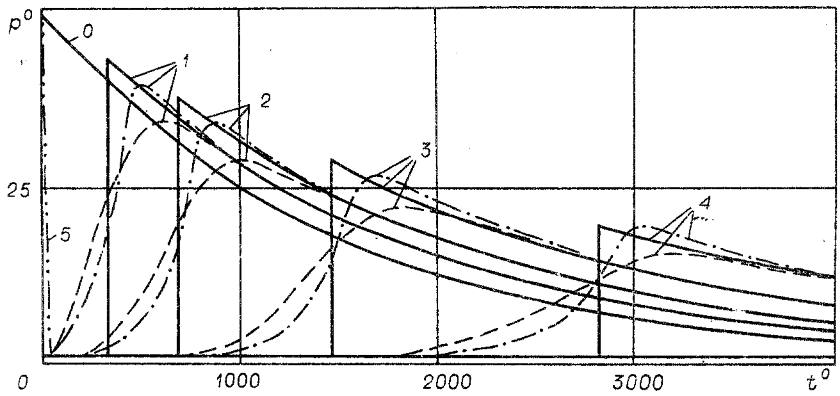

Fig. 3

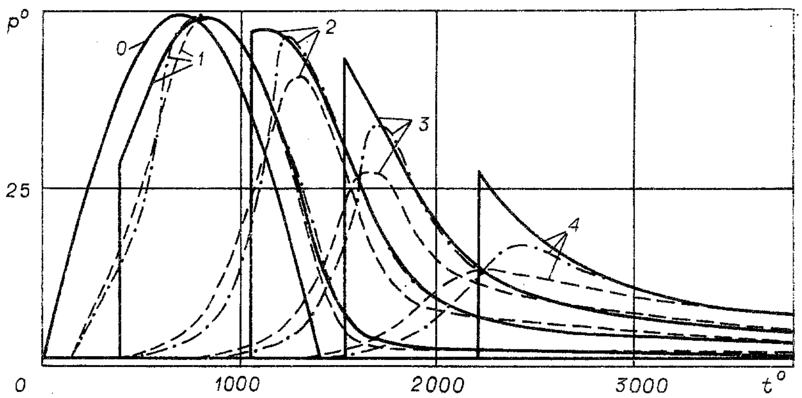

Fig. 4

mum pressures for constant, variable, and zero η here also do not exceed 15-25%. The greatest damping of the maximum pressure with distance is observed for variable η, and the smallest for an inviscid medium. An increase in the air content leads to an increase in the wave damping, as was noted earlier [1, 6].

Let us consider the propagation of a wave generated by the continuously varying load described by (10) (half-period of a sinusoid) for $p^\circ = 50$ and $\theta^\circ = 1400$. The air content in water $\alpha_1 = 0.01$. The results of the calculation are shown in Fig. 4. Curves 0-4 determine p(t) in cross sections of the medium where $x^\circ = 0$, 100, 350, 550, and 800 respectively during the passage of a wave. As before, the solid curves refer to an inviscid medium, the dash-dot curves to a constant η, and the dashed curves to a variable η.

A wave having a jump at the front is generated in an inviscid medium near the initial cross section; to start with, the magnitude of the jump is infinitesimal. Behind the jump the pressure increases continuously to a maximum. As the wave propagates, the magnitude of the jump at the front is increased, and the magnitude of the following continuous pressure increase is diminished. At a certain distance the wave is transformed into a pure shock wave with the pressure maximum at the jump and lower behind it. With further propagation the maximum pressure decreases, and the duration of the wave increases. The transformation of a continuous wave into a pure shock ends rather quickly. During the transformation the maximum pressure decreases by less than 10%.

Neglecting viscosity, the compressibility diagram of water containing gas bubbles corresponds to $V_S^\circ(p^\circ)$ in Fig. 2, and the compressibility diagram of pure water coincides with $V_D^\circ(p^\circ)$. In both media these curves are convex to the origin of coordinates, and therefore continuous waves are transformed into shocks. However, the curvature of the V(p) diagram for water containing bubbles is significantly greater than that for pure water, and therefore effects connected with curvature appear more strongly.

In viscous media (cf. Fig. 4) smearing of the continuous wave is observed, and the time between the arrival of the beginning of the disturbance and its maximum increases as the wave propagates. Simultaneously with the smearing in certain parts ($x^\circ = 100\text{-}350$), the profile of p(t) becomes steeper (in the region of increasing pressure), and the wave gradually approaches a shock. At large distances the inverse process begins — the slope decreases ($x^\circ = 550\text{-}800$) and the profile becomes less steep. The smearing of the wave and the increase in slope of the profile occur for constant and variable η.

The smearing of the wave is related to the viscous properties of the medium, and the increase in slope to the nonlinearity of the static compression diagram. When this diagram is linear, there is no increase in slope of the profile [7]. The smearing of a continuous wave generated by sinusoidal loading in glycerin containing air bubbles, and a simultaneous increase of the slope of the profile in a certain part, were found experimentally in [8, 9].

The differences of the maximum pressures in a wave generated by a continuously varying load with and without taking account of viscosity reach 50%, and for constant and variable η 20%. The p(V) curves for constant and variable η obtained in various cross sections of the medium during the passage of a wave are negligibly different, as in the case of impact loading (cf. Fig. 2).

Thus, taking account of bulk viscosity in the model of a medium leads to a change in the character of the wave-smearing of the profile, the creation of two maxima, the delay of the development of deformations relative to the pressure, and a change in the rate of damping with distance. The wave profile may become steeper in certain parts.

The introduction of a variable instead of a constant viscosity does not change the general character of the wave, but leads to an increase in the rate of damping and the smearing of the wave with distance. An increase in pressure from 10^5 to 50×10^5 N/m^2 is accompanied by a decrease in the equilibrium radius of a bubble by a factor of 2.53, the volume of the gaseous component by 16.33, and the viscosity η by 6.44. For this change in η the rate of damping and the smearing of the wave increase by only 10-20%. This shows that approximate values of the bulk viscosity can be used in solving wave problems in the cases considered.

LITERATURE CITED

1. G. M. Lyakhov and V. N. Okhitin, "Spherical blast waves in multicomponent media," Prikl. Mekh. Tekh. Fiz., No. 2 (1974).
2. B. R. Parkin, F. P. Gilmore, and G. L. Broud, "Shock waves in water containing gas bubbles," in: Underwater and Underground Explosions [Russian translation], Mir, Moscow (1974).
3. V. A. Plaksii, "Cylindrical detonation waves in multicomponent media," Zh. Prikl. Mekh. Tekh. Fiz., No. 3 (1978).
4. G. M. Lyakhov and V. N. Okhitin, "Nonstationary plane waves in media with bulk viscosity," Zh. Prikl. Mekh. Tekh. Fiz., No. 5 (1977).
5. G. M. Lyakhov and V. N. Okhitin, "Spherical detonation waves in media with bulk viscosity," Zh. Prikl. Mekh. Tekh. Fiz., No. 6 (1977).
6. G. M. Lyakhov, Fundamentals of the Dynamics of Blast Waves in Soils and Rocks [in Russian], Nedra, Moscow (1974).
7. G. M. Lyakhov and K. S. Sultanov, "Longitudinal waves in linear viscoelastic media," Izv. Akad. Nauk SSSR, Fiz. Zemli, No. 8 (1978).
8. L. G. Grebenkina, G. A. Druzhinin, and A. S. Tokman, "Distortion of compression pulse shapes during propagation in a porous liquid," in: Data from Ninth All-Union Acoustic Conf. [in Russian], Moscow (1977).
9. G. A. Druzhinin, G. A. Ostroumov, and A. S. Tokman, "Nonlinear reflection of shock waves and shock curves of liquids with gas bubbles," in: Data of Symposium on Nonlinear Strain Waves [in Russian], Tallin (1978).